# CHAPTER 8. CONCLUDING REMARKS AND SOME SUGGESTIONS FOR FURTHER RESEARCH

## 8.1 Sferics correlations

In order to reduce sferics noise with neural network-based prediction filters, it is necessary to understand the correlation between orthogonal components of sferics noise and the spatial correlation of sferics noise in both horizontal and vertical planes. Three-component sferics correlation measurements were carried out at four areas (i.e., Ku-Ring-Gai National Park, Mt Isa, Darwin, and Parkes).

One-second time pulses derived from a Global Positioning System (GPS) were used to synchronise sferics measurements at two station with various separations. For measurements of the correlation of the three components of sferics noise at frequencies above 5 kHz, a SIROTEM receiver coil (RVR-3C) was used. Horizontal-axis induction coils (called Drovers) and a two-turn 100m×100m loop were used to measure the horizontal (X and Y) components and the vertical (Z) component of low-frequency (<1 kHz) sferics noise, respectively.

Low-frequency sferics measurements of each component were made with a 10 kHz anti-aliasing filter placed at the input of the preamplifiers, and a 1 kHz filter at the output of the preamplifier.

Generally, it is concluded that there is close correlation between the three components of high-frequency sferics noise measured at a given station, and between corresponding components measured at two stations separated by distances up to 11 km. The largest dispersion effect caused by a difference in ground conductivity at two separated stations can be seen on the vertical component of sferics noise.

Simultaneous horizontal-component measurements of low-frequency sferics at two separated receivers show a high degree of correlation and nearly no time shift between corresponding sferics pulses even when the receivers are separated by a distance of 11 km.

Twenty-four hour monitoring of sferics at Ku-Ring-Gai National Park has shown that there are two periods of minimum activity each day. For example, during one such measurement period, minima were recorded from 6:00 AM to 1:30 PM and from 6:30 to 10:30 PM. While more extensive monitoring is required to determine variations with latitude and time of year, these times can be used as guidelines for best times to carry out airborne electromagnetic (AEM) surveys. The sferics count rates during these minimum activity periods are about 3 to 9 times smaller than those during the rest of the day. These lower count rates imply that the stacking time for AEM measurements can be reduced by a factor of 3 to 9 to obtain the same data quality as an AEM survey carried out during a period of maximum sferics activity.

### 8.2 Neural network-based noise reduction filters

Noise prediction filters using neural networks differ from most applications of neural networks for classification problems (e.g., determination of crop types from satellite photographs and handwriting recognition) and data (image) compression. Real value (continuous)-output neural networks have been used for noise reduction instead of binary (discrete)-output networks normally used for classification. In real-value applications of a neural network with a hyperbolic tangent as an activation function, the output values are theoretically limited to an output range of -1 to 1. In order to achieve these values, the weighted summation at any PE in the network should theoretically be infinite. In practice, the output values from the network are scaled in a range of -0.9 to 0.9 at most. This scaling implies that small errors in the network calculation during training become much larger for the corresponding unscaled values. It is therefore necessary that, in real-value applications of neural networks, the network must be trained to near-perfection in order to have small, unscaled output errors. However, in most classification applications of a (binary output) neural network, values of -0.9 and 0.9 can be considered equivalent to 0 and 1, respectively.

### 8.2.1 Model training method

A model training method (MTM) has been used to predict a noise-free transient using a neural network trained with forward model calculations of the TEM response of a range of layered-earth models. A neural network was configured with 20 processing elements (PE) in the input and output layers and 40 PEs in a single hidden layer. A hyperbolic tangent was used as an activation function in the hidden and output layers of the network. The output values were scaled in a narrow range (-0.8 to 0.8) near the center of the network's limits. This linearising of the network is not a serious problem, as hidden layers can still operate over their full nonlinear range, which is all that is mathematically required.

It has been demonstrated that an MTM can filter out spike-like EM noise from a noisy transient and can produce a noise filter error (NFE) of less than 17% at late delay times. Also, comparison between an MTM and a least-square fitting method shows that the MTM reduces noise by a factor of 2.5 greater than the least-square method. However, an MTM cannot be generally applied, since the method is model dependent. Therefore, the use of this method would be limited to curves where training can be applied with a range of enough models to cover the geological structure of a given region where EM data are being collected.

However, there are limits beyond which a given network will fail to learn as Minsky and Papert (1988) have pointed out for a linear neural network (e.g., a perceptron network). The magnitude of the parameters of a perceptron is not the only source of this scaling failure, and another source involves the size, or rather the information content, of the weight coefficients. The scaling problem is not unique to the linear network and arises in real-value applications of a backpropagation network. The backpropagation network encounters longer and more difficult training sessions as the scope of the problem is scaled up. In an MTM, the scale of the problem increases exponentially as the training region (i.e., the size of the training set) increases. For example, if a dynamic range of $10^6$ at each delay time of a training region is scaled in an output range of -0.8 to 0.8 mentioned in the previous section, the number of hidden processing elements (PEs) and the number of cycles needed for learning to converge dramatically increase.

In order to avoid this scaling problem occurring in the application of an MTM, further study of the MTM should be performed. One approach is to break a complex and large problem into several smaller toy-scale problems through the use of multiple networks referred to as a modular neural network by Poulton and Birken (1995).

### 8.2.2 Noise prediction filters

A neural network-based local noise prediction filter (LNPF) has been used to predict the vertical component of EM noise from the two horizontal components measured simultaneously. A neural network was configured with 102 PEs in the input, one PE in the output layer, and no hidden layer. A hyperbolic tangent was used as the activation function in the output layer of the network. The output values were scaled to a range of -0.8 to 0.8.

For the reduction of VLF (e.g., 10, ~20, and 44 kHz), high-frequency (>~5 kHz) sferics, and low-frequency (<~1 Hz) geomagnetic field variations, a neural network-based LNPF achieves an NRF of more than 5 and consistent performance over time (stationarity). For high-frequency sferics pulses, the LNPF suppresses sferics power by 20 dB (i.e., an NRF of 10 in amplitude) when only sferics power reduction is considered in a frequency range of 5 to 50 kHz, where power from sferics pulses is generally measured with an RVR-3C.

The neural network-based LNPF has been compared with the Spies LNPF based on the tipper method. For reduction of low-frequency geomagnetic field variations, the neural network-based LNPF and the Spies LNPF with a 48-point filter length achieve nearly the same performance. However, the Spies LNPF needs more than 5 times longer computation time than the neural network method. For high-frequency sferics reduction, the Spies method with a 24-point filter length is worse than the neural network method when the sferics pulse has approximately equal amplitudes in both the X and Y components. In cases where the sferics pulse is polarised mainly along the X or Y direction, the two methods achieve almost same performance.

The application of a neural network-based LNPF has been assessed with ground-based TEM measurements made in exploration conditions. Measurements of TEM responses with an in-loop geometry were made at a mineral prospect near Parkes in August, 1995. Smooth TEM profiles were obtained by applying the LNPF compared with the profiles obtained without applying the LNPF. When the LNPF was applied to the in-loop TEM data, the network coefficients were updated with new sferics noise every two stations (i.e., a distance of 100 m). With this adaptation procedure, the neural network shows good performance at most stations. However, in areas where the ground conductivity changes from station to station (e.g., near a mineralised zone), the performance of the neural network method is significantly reduced and the network needs to be completely retrained.

Since Parkes data show that the sferics activity was very low (i.e., 6 sferics pulses per sec), the neural network-based LNPF has been applied to very high sferics activity data (i.e., 76 sferics pulses per sec) added to transient responses measured at Parkes. In this application, an NRF value of 3.4 was obtained from calculating the RMS of the average of fifty 20-ms bipolar stacks of the noise without use of the LNPF and dividing by the corresponding average obtained by stacking after applying the LNPF to each bipolar stack.

A remote noise prediction filter (RNPF) has been tested with separations between the local (primary) receiver and remote receiver varying from 1 to 11 km. The nonlinearities were located in the activation function of the hidden PEs for the reduction of high-frequency sferics. For the reduction of background noise, nonlinearities were located in both hidden and output PEs. Such a filter produces a reduction of background EM (VLF) noise by 20 dB (i.e., an NRF of 10 in amplitude). For the horizontal (X and Y) component reduction of high-frequency sferics, the RNPF attenuates the power of sferics noise by more than 25 dB (i.e., by a factor of 18 in amplitude) at frequencies in the range of 5 to 50 kHz, where power is contributed by sferics.

For reduction of the vertical component of sferics, the dispersion effect caused by a variation in ground conductivity between the two separated stations makes it difficult for the neural network to recognise the amplitude change and time shift between the two Z component of sferics pulses at the local and remote stations. In this case, the performance of an RNPF is improved when an LNPF concept is applied. For such filter, a neural network has been configured to predict the local Z-component sferics using all three components of corresponding sferics at the remote station. This filter has been referred to in this thesis as an XYZ-RNPF.

In the comparison between an RNPF and simple subtraction, it is shown that the RNPF is superior to simple subtraction of the remote time series from the local one in the reduction of all three components of sferics. The performance of an autoregressive moving average model (a transfer function model) is worse when the residual time shift is different from the residual time shift between the local and remote sferics time series used in the training of the transfer function model. Otherwise, the performance of the transfer function model is only marginally worse than the performance of the neural network-based RNPF. On the other hand, the RNPF gives a consistently better performance because it is trained to accommodate different residual time shifts between the two series.

An RNPF has been applied to ground-based TEM measurements made in exploration conditions. Measurements of the three-component TEM responses with a fixed-loop geometry were made at a mineral prospect near Parkes, 1995. The RNPF produces smooth TEM profiles. When the RNPF was applied to the fixed-loop TEM data, the network coefficients trained at the previous station were adjusted with new sferics noise measured at the present station. At all stations, the RNPF for reduction of the X and Y components of sferics noise gives good performance. However, the network for reduction of the Z component of sferics noise has to be completely retrained near a mineralised zone.

The RNPF has also been evaluated with high sferics activity (i.e., 86 sferics pulses per sec) data recorded simultaneously at two stations with 1 km separation in Darwin in December 1994. It was found that the RNPF reduced sferics noise by a factor of 4.7 when the RMS of the average of fifty 20-ms bipolar stacks of the noise without the use of the RNPF was divided by the corresponding average obtained after applying the RNPF.

In order to improve the signal-to-noise (S/N) ratio at a late time, most TEM systems use a windowing scheme. This windowing scheme can achieve good noise reduction only when the peak of a given sferics pulse occurs near the centre of an applied window and the width of the applied window is enough wide to cover this sferics pulse. Otherwise, a high S/N ratio at late delay times cannot be obtained by applying the windowing scheme. Referring to Figures 6.3 and 7.12, low-frequency noise (depends on the width of the applied window ) is produced by the windowing scheme when it is applied to high-frequency sferics noise. This disadvantage of the windowing scheme emphasises the fact that to obtain a good S/N ratio at late times (see Figures 7.13 and 7.23), high-frequency sferics noise should be reduced before stacking and applying the windowing scheme to a noisy transient.

For practical implementation of noise prediction filters (LNPF and RNPF), an automatic method for determining the occurrence of sferics is required. The brute force method described in Section 2.2 for detection of sferics pulses greater than background noise level is very effective but this method cannot be used to recognise sferics pulses just above or below background noise level or, more importantly, when TEM signal is present. Automatic recognition of the occurrence of sferics pulses is required. This automatic detection of sferics pulses could possibly be accomplished with wavelet analysis (Meyer and Ryan, 1993) and neural networks.

Real-time application of an RNPF to rejection of high-frequency sferics noise presents two main difficulties. Firstly, noise data measured at the remote station has to be transferred in real time with either telemetry or a wire link between the local and remote stations. A wire link cannot be used for AEM system and would limit the separation between local and remote stations for ground-based TEM methods. With telemetry, remote reference data will be lost whenever communication between the local and remote receiver fails. Secondly, the number of operations and calculations (e.g., the determination of the occurrence of sferics pulses, transfer of noise data measured at the remote station, and calculation of cross-phase spectrum) required to determine the time shift between high-frequency components of corresponding sferics pulses measured at the local and remote stations is extremely large. Without the introduction of an expensive parallel processing procedure, involving up to five independent computers at both the local and remote stations to handle the various operations, it would not be possible to apply an RNPF in real time. Therefore, application of an RNPF for reduction of high-frequency sferics noise in ground-based TEM and AEM measurements is at present practical only as a post-processing procedure.

To minimise computer memory and storage space required to apply the an LNPF and RNPF to non-windowed time series, it would be desirable to investigate whether the noise prediction filters can be applied effectively after windowing and stacking of a given response. When the horizontal component has a large signal caused by lateral changes in conductivity, it would be valuable to investigate an LNPF which predicts the vertical component of noise using the two horizontal components applied by a first-order difference method (as described in Section 7.2.2.1).

We have set up a remote receiver at sufficient distance from a local receiver such that no transmitter primary signal is detectable. Remote referencing where reference is too close and contains some TEM signal has not been studied but would be very worthwhile to remove noise from power lines near the primary receiver.

# REFERENCES


Ahalt, S.C., Garber, F.D., Jouny, I., and Krishnamurthy, A.K., 1989, Performance of synthetic neural network classification of noisy radar signals: Advances in Neural Information Processing Systems, **1**, Morgan Kaufmann Publishers, San Mateo, CA, 281-288.

Ahmad, S., and Tesauro, G., 1989, Scaling and generalization in neural networks: A case histroy: Advances in Neural Information Processing Systems, **1**, Morgan Kaufmann Publishers, San Mateo, CA, 160-168.

Aleksaunder, I., and Martin, H., 1989, An introduction to neural computing: Chapman and Hall.

Alvelda, P., and Martin, A.M.S., 1989, Neural networks star pattern recognition for spacecraft attitude determination and control: Advances in Neural Information Processing Systems, **1**, Morgan Kaufmann Publishers, San Mateo, CA, 315-322.

Anderson, J., and Rosenfeld, E., 1989, Neurocomputing: Foundations of research: MIT Press.

Asten, M.W., and Price, D.G., 1985, Transient EM sounding by in/out-loop method: Exploration Geophysics, **16**, 165-333.

Bahl, L.R., Brown, P.F., de Souza, P.V., and Mercer, R.L., 1987, Speech recognition with continuous-parameter hidden Markov models: Computer Speech and Language, **2**, 219-234.

Balser, M. and Wagner, C.A., 1960, Observations of earth-ionosphere cavity resonances: Nature, **188**, no. 19, 638-641.

Baum, E.B., and Haussler, D., 1989, What size net gives valid generalization ?: Advances in Neural Information Processing Systems, **1**, Morgan Kaufmann Publishers, San Mateo, CA, 81-90.

Becker, S.B., and Le Cun, Y., 1988, Improving the convergence of back-propagation learning with second-order methods: Proceedings of the 1988 Connectionist Models Summer School, San Mateo, Morgan Kaufman, 29-37.

Bennett, R.J., 1979, Spatial time series: Analysis-Forecasting-Control: Pion Limited, 207 Brondesbury Park, London NW2 5JN.

Berdichevskiy, M.N., 1965, Electrical prospecting with the telluric current method: Colorado School of Mines, **60**, no. 1, 48-49.

Box, G.P., 1976, Time series analysis: forecasting and control: Holden-Day, San Francisco.

Brent, R.P., 1991, Fast training algorithm for multilayer neural nets: IEEE trans. on Neural Networks, **2**, 346-354.

Buselli, G., 1977, Transient electromagnetic measurements to late delay times over the Woodlawn ore body: Bull. Aust. Soc. Explor. Geophys., **8**, no. 1, 1-5.

Buselli, G., and Cameron, M.A., 1992, Improved sferics reduction in TEM measurements: CSIRO Division of Exploration Geoscience, Restricted Report 273R (now on open file), 60 pp.

Buselli, G., and Cameron, M.A., 1993, Final report for AMIRA Project P250A: Improved TEM detection of massive sulphide orebodies: Restricted Report 350R (now on open file), 29 pp.

Buselli, G., and Cameron, M.A., 1995, Robust statistical methods for reducing sferics noise contaminating transient electromagnetic measurements: Submitted to Geophysics.

Buselli, G., and O'Neill, B., 1977, SIROTEM: A new portable instrument for multichannel transient electromagnetic measurement: Bull. Aust. Soc. Explor. Geophys., **8**, no. 3, 82-87.

Cagniard, L., 1953, Basic theory of the mahnetotelluric method of geophysical prospecting: Geophysics, **18**, 605-635.

Cary, P., and Upham, W., 1992, An evaluation of neural networks: Geophysics: The Leading Edge of Exploration, September, 45-47.

Caudill, M., 1988, Neural Networks Primer, Part IV, AI Export, August, 61-67.

Chan, L.-W., and Fallside, F., 1987, An adaptive training algorithm for backpropagation networks: Computer Speech and Language, **2**, 205-218.

Chauvin, Y., 1989, A back-propagation algorithm with optimal use of hidden units: Advances in Neural Information Processing Systems, **1**, Morgan Kaufmann Publishers, San Mateo, CA 519-526.

Clarke, J., Gamble, T.D., Goubau, W.M., Koch, R.H., and Miracky, R.F., 1983, Remote-reference magnetotellurics: equipment and procedures: Geophysical Prospecting, **31**, 149-170.

Cybenko, G., 1989, Approximation by superpositions of a sigmoidal function: Math. Control Signals Systems, **2**, 303-314.

Davalo, E., and Naim, P., 1991, Neural networks: Editions Eyrolles, Paris.

Dayhoff, J., 1989, Neural Network Architectures: Van Nostrand Reinhold, New York, NY.

Denker, J.S., Gardner, W.R., Graf, H.P., Henderson, D., Howard, R.E., Hubbard, W., Jackel, L.D., Baird, H.S., and Guyon, I., 1989, Neural network recognizer for hand-written zip code digits: Advances in Neural Information Processing Systems, **1**, Morgan Kaufmann Publishers, San Mateo, CA, 323-331.

Ernst, T., 1981, A comparison of two methods of the transfer function calculation using the least-square criterion in time and frequency domain: Publ. Inst. Geophys. Pol. Acad. Sci., **G-2**, no. 143, 13-24.

Fahlman, S.E., 1988, Faster-learning variations on backpropagation: An empirical study: Proceedings of the 1988 Connectionist Models Summer School, Morgan Kaufmann Publishers, San Mateo, CA.

Fahlman, S.E., and Lebiere, C., 1989, The cascade-correlation learning architecture: Advances in Neural Information Processing Systems, **2**, Morgan Kaufmann Publishers, San Mateo, CA, 524-532.

Fossati, M., Zerilli, A, Ronchini, G., and Apolloni, B., 1992, Lineaments analysis for potential-fields data using neural networks: The SEG Sixty-second Annual International Meeting and Exposition, 6-9.

Gamble, T. D., Goubau, W.M., and Clarke, J., 1979a, Magnetotellurics with a remote magnetic reference: Geophysics, **44**, 53-68.

Gamble, T. G., Goubau, W.M., and Clarke, J., 1979b, Error analysis for remote reference magnetotellurics: Geophysics, **44,** 959-968.

Gori, M., and Tesi, A., 1992, On the problem of local minima in backpropagation: IEEE trans. on Pattern Analysis and Machine intelligence, **14**, 76-86.

Goubau, W. M., Maxton, P.M., Koch, R.H., and Clarke, J., 1984, Noise correlation lengths in remote reference magnetotellurics: Geophysics, **49,** 433-438.

Gu, M.X., Pao, Y.H., and Yip, P.P.C., 1993, Neural-net computing for real-time control of a ship's dynamic positioning at sea: Control Eng. Practice, **1**, no. 2, 305-314.

Guo, Y., Hansen, R.O., and Harthill, N., 1992, Feature recognition from potential fields using neural networks: The SEG Sixty-second Annual International Meeting and Exposition, 1-5.

Halverson, M.O., 1982, Telluric noise cancellation in induced polarization prospecting: U.S.patent No. 4339720.

Halverson, M.O. 1990, Real-time telluric cancellation in broadband IP exploration: Fink, J.B., McAlister, E.O., Sternberg, B.K., Wieduwilt, W.G., and Ward, S.H., Eds., Induced polarization-Applications and case histories: Investigations in Geophysics, Vol. 4, SEG, 199-226.

Halverson, M.O., Kingman J.E.E., and Corbett, J.D., 1987, Advances in IP technology: Telluric cancellation and high spatial resolution arrays: Exploration 87 proceedings, 183-190.

Hanson, S.J., and Pratt, L.Y., 1989, Comparing biases for minimal network construction with back-propagation: Advances in Neural Information Processing Systems, **1**, Morgan Kaufmann Publishers, San Mateo, CA, 177-185.

Hinton, G.E., 1989, Connectionist learning procedures: Artificial Intelligence, **40**, no. 1, 143-150.

Hornik, K., Stinchcombe, M., and White, H., 1989, Multilayer feedforward networks are universal approximators: Neural networks, **2**, 359-366.

Huang, K.Y., and Liaw, J.Y., 1992, Neocognition of a neural network for seismic pattern recognition: The SEG Sixty-second Annual International Meeting and Exposition, 26-29.

Huang, W.M., and Lippmann, R.P., 1988, Neural net and traditional classifiers: Neural Information Processing Systems, American Institute of Physics, New York, 387-396.

Jacobs, R.A., 1988, Increased rates of convergence through learning rate adaptation: Neural networks, **1**, 295-307.

Jasic, T., and Poh, H.L., 1995, Financial time-series prediction using neural networks: a case study for the TOPIX data: Proceedings of the Sixth Australian Conference on Neural Networks, 65-68.

Kemp, F., Threet, J.R., and Veezhinathan, J., 1992, A neural net branch and bound seismic horizon tracker: The SEG Sixty-second Annual International Meeting and Exposition, 10-13.

Kim, B.O., and Hohmann, G.W., 1992, Adaptive noise cancellation for time domain EM data: Geophysics, **57**, 466-469.

Labson, V.F., Becker, A., Morrison, H. F., and Conti, U., 1985, Geophysical exploration with audiofrequency natural magnetic fields: Geophysics, **50**, 656-664.

Lang, K.J., and Hinton, G.E., 1989, Dimensionality reduction and prior knowledge in E-set recognition: Advances in Neural Information Processing Systems, **2**, Morgan Kaufmann Publishers, San Mateo, CA, 178-185.

Lapedes, A., and Farber, R., 1987, Nonlinear signal processing using neural networks: Prediction and sytem modelling: Technical Report, Los Alamos National Laboratory, Los Alamos, New Mexico.

Lapedes, A., and Farber, R., 1988, How neural nets work: Neural Information Processing Systems, New York, American Institute of Physics, 442-456.

Le Cun, Y., Denker, J.S., and Solla, S.A., 1990, Optimal brain damage: Advances in Neural Information Processing Systems, Morgan Kaufmann Publishers, San Mateo, CA, 599-605.

Lee, J., Weger, R.C., Sengupta, S.K., and Welch, R.M., 1990, A neural network approach to cloud classification: The IEEE transactions on Geoscience and Remote Sensing, **28**, no. 5, 846-855.

Lippmann R.R., 1987, An introduction to computing with neural nets: IEEE ASSP magazine, **4**, no. 2, 4-22.

Lippmann, R.P., and Becckman, P., 1989, Adaptive neural net preprocessing for signal detection in non-gaussian noise: Advances in Neural Information Processing Systems, **1**, Morgan Kaufmann Publishers, San Mateo, CA, 125-131.

Lorenzetti, E.A., 1992, Predicting lithology from Vp and Vs using neural networks: The SEG Sixty-second Annual International Meeting and Exposition, 14-17.

Lowe, D., and Webb, A., 1989, Adaptive networks, dynamical systems, and the predictive analysis of time series: Controller HMSO, London, 95-99.

Macnae, J.C., Lamontage, Y., and West, G.F., 1984, Noise processing techniques for time-domain EM systems: Geophysics, **49**, 934-948.

Malkoff, D.B., 1989, A neural network for real-time signal processing: Advances in Neural Information Processing Systems, **2**, Morgan Kaufmann Publishers, San Mateo, CA, 248-255.

Malkoff, D.B., and Cohen, L., 1990, A neural network approach to the detection problem using joint time-frequency distributions: Proceedings of the IEEE 1990 International Conference on Acoustics, Speech, and Signal Processing, New Mexico, 2739-2749.

Masters, T., 1993, Practical neural network recipes in C++: Academic Press, Inc.

McClelland, J.L., and Rumelhart, D.E., 1988, Explorations in Parellel Distributed Processing: MIT Press.

McMechan, G.A., and Barrodale, I., 1985, Processing electromagnetic data in the time domain: Geophys. J. Roy. Astr. Soc., **81**, 277-293.

Meyer, Y., and Ryan R.D., 1993, Wavelets: Algorithm and Applications: SIAM, Philadelpia, 1993.

Minsky, M., and Papert, S., 1988, Perceptrons: An introduction to computational geometry: MIT press, Cambridge, MA.

Morgan, N., and Bourland, H., 1989, Generalization and parameter estimation in feedforward nets: Some experiments: Advances in Neural Information Processing Systems, **2**, Morgan Kauffmann, Publisher, 630-633.

Moody. J., 1989, Fast learning in multi-resolution hierarchies: Advances in Neural Information Processing Systems, **1**, Morgan Kauffmann, Publisher, 29-39.

Moody, J., and Darken, C.J., 1988, Learning with localized receptive fields: Proceedings of the 1988 Connectionist Models Summer School, Morgan-Kauffmann, Publishers.

Moody, J., and Darken, C.J., 1989, Fast learning in networks of locally-tuned processing units: Neural computation, **1**, No. 2, 281-294.

Nichols, E.A., and Morrison, H.F., 1988, Signals and noise in measurements of low-frequency geomagnetic fields: Journal of Geophysical Research, **93**, no. B11, 13743-13754.

Pao, Y.H., 1989, Adaptive pattern recognition and neural networks: Addison-Wesley Publishing Co., Inc., MA.

Pao, Y.H., Phillips, S.M., and Sobajic, D.J., 1992, Neural-net computing and the intelligent control of systems: International Journal of Control, **56**, no.2, 263-289.

Park, C.G., 1982, Whistlers: CRC Handbook of Atmospherics, **2**, CRC press, Inc., 21-77.

Park, C.G., and Helliwell, R.A., 1978, A magnetospheric effect of power line radiation: Science, **200**, 727.

Park, D.C., El-Sharkawi, M.A., and Marks II, R.J., 1991, An adaptively trained neural network: IEEE transactions on neural networks, **2**, 334-345.

Park, G.H., 1990, System identification and noise cancellation with neural networks: M.S. thesis, Electrical Engineering, Case Reserve University, Cleveland, Ohio.

Pierce, E.T., 1977, Atmospherics and radio noise: Academic Press, 351-384.

Pineda, F., 1988, Generalization of backpropagation to recurrent and higher order networks: Neural Information Processing Systems, American Institute of Physics, New York, 602-611.

Polk, C., 1982, Schumann resonances: CRC Handbook of Atmospherics, **1**, CRC press, Inc., 111-178.

Poulton, M.M., and Birken, R.A., 1995, Estimating one-dimensional models from frequency-domain electromagnetic data using modular neural networks: Submitted to IEEE Geoscience and Remote Sensing.

Poulton, M.M., Sternberg, B.K., and Glass, C.E., 1992a, Location of subsurface targets in geophysical data using neural networks: Geophysics, **57**, no. 12, 1534-1544.

Poulton, M.M., Sternberg, B.K., and Glass, C.E., 1992b, Neural network pattern recognition of subsurface EM images: Journal of Applied Geophysics, **29**, 21-36

Principe, J.C., and Zahalka, A., 1994, Transient signal detection with neural networks: The search for the desired signal: Advances in Neural Information Processing Systems, **6**, Morgan-Kauffmann, Publisher, 685-695.

Richmond, A.D., 1986, Upper-atmosphere electric-field sources: The Earth's Electrical Environment, National Academy Press, Washington, DC.

Robinson, E.A., 1967, Predictive decomposition of time series with application to seismic exploration: Geophysics, **34**, 75-86.

Roth, G., and Tarantola, A., 1992, Inversion of seismic waveforms using neural networks: The SEG Sixty-second Annual International Meeting and Exposition, 788-791.

Rumelhart, D.E., Hinton, G.E., and Williams, R.J., 1986a, Learning internal representations by error propagation: Parallel distributed processing, Exploration in the Microstructures of Cognition, **1**, MIT Press, Cambridge, MA.

Rumelhart, D.E., Hinton, G.E., and Williams, R.J., 1986b, Learning representations by back-propagating errors: Nature, **323**, 533-536.

San Filipo, W.A., and Hohmann, G.W., 1983, Computer simulation of low frequency electromagnetic data acquisition: Geophysics, **48**, 1219-1232.

Schmidt, J., Brazil, P, and Hadsell, F.A., 1992, Neural network stacking velocity picking: The SEG Sixty-second Annual International Meeting and Exposition, 18-21.

Schmidt, K., and Cull, J., 1995, Application of Euler deconvolution and a neural network system as interpretation aids for three component downhole TEM data: Exploration Geophysics, **26**, 154-157.

Smith, R.S., and West, G.F., 1988, TEM coincident loop negatives and the loop effect: ASEG/SEG Conference-Adelaide, 354-357.

Spies, B.R., 1988, Local noise prediction filtering for central induction transient electromagnetic soundings: Geophysics, **53**, 1068-1079.

SPLUS, 1993, Statistical Sciences, Inc., Seattle, Washington.

Stephan, A., and Strack, K.-M., 1990, A simple approach to improve the S/N ratio for TEM data using multiple receivers: Submitted to Geophysics.

Stornetta, W.S., and Huberman, B.A., 1987, An improved three-layer, back propagation algorithm: Proceedings of the IEEE First International Conference on Neural Networks, San Diego, CA.

Strack, K.-M., Hanstein, T.H., and Eilenz, H.N., 1989, Lotem data processing in areas with high cultural noise level: Phys. Earth Plan. Int., **53**, 261-269.

Sumner, J.S., 1976, Principles of induced-polarization: Elsevier Science Publishing Company, Oxford, New York, 135-145.

Sutton, R.S., 1986, Two problems with backpropagation and other steepest-descent learning procedures for networks: Proceedings of the 8th Annual Conference of the Cognitive Science Society, 823-831.

Tamura, S., and Waibel, A., 1988, Noise reduction using connection models: Proceedings of the IEEE International Conference on Acoustics, Speech and Signal Processing, **1**, 553-556.

Tikhonov, A.N., 1950, On determining electrical characteristics of the deep layers of the earth's crust: Doklady, **73**, 292-297 (Reprinted in Magnetotelluric methods: Geophys. Reprint Ser., No.5, edited by K. Vozoff, SEG, Tulsa, Okla., 1986).

Vozoff, K., 1972, The magnetotelluric method in the exploration of sedimentary basins: Geophysics, **37**, 98-141.

Vozoff, K., 1984, Regions of anomalously large telluric interference in IP: The Cobar Syndrome: Exploration Geophysics, **15**, 175-178.

Vozoff, K., and Ellis, R.M., 1966, Magnetotelluric measurements in southern Alberta: Geophysics, **37**, 281-289.

Wait, J.R., 1970, Electromagnetic Waves in Stratified Media: Pergamon Press, Oxford.

Ward, S.H., 1967, The electromagnetic method: Mining Geophysics, Vol. II, Society of Exploration Geophysicists publication, 224-372.

Wasserman, P., 1989, Neural Computing: Theory and Practice: Van Nostrand Reinhold, New York.

Weigend, A.S., Rumelhart, D.E., and Huberman, B.A., 1990a, Back-propagation, weight-elimination and time series prediction: Connectionist Model, **1**, 105-117.

Weigend, A.S., Rumelhart, D.E., and Huberman, B.A., 1990b, Predicting the future: A connectionist approach: International Journal of Neural Systems, **1**, no. 3, 193-209.

Werbos, P., 1974, Beyond regression: New tools for prediction and analysis in the behavioral sciences: PhD. Thesis, Harvard University.

Widrow, B., 1987, ADALINE and MADALINE: Proc. IEEE 1st Intl. Conf. on Neural Networks, Vol. I, 143-158.

Widrow, B., Glover, O.R., McCool, J.M., Kaunitz, J., Williams, C.S., Hearn, R.M., Zeidler, J.R., Dong, Jr., E., and Goodlin, R.C., 1975, Adaptive noise cancelling: Principles and applications: Proceedings of the IEEE, **63**, 1672-1716.

Widrow, B., McCool, J.M., Larimore, M.G., and Johnson, Jr, C.R., 1976, Stationary and nonstationary learning characteristics of the LMS adaptive filter: Proceedings of the IEEE, **64**, 1151-1162.

Widrow, B., and Sterns, S.D., 1985, Adaptive signal processing: Prentice Hall, Inc.

Widrow, B., Winter, R.G., and Baxter, R.A., 1988, Layered neural nets for pattern recognition: IEEE Transactions on Acoustics, Speech, and Signal Processing, **36**, no. 7, 1109-1118.

Wieladek, R., and Ernst, T., 1977, Application of the method of least squares to determining impulse responses and transfer functions: Publ. Inst. Geophys. Pol. Acad. Sci., **G-1**, no. 110, 3-12.

Wilt, M., Goldstein, N.E., Stark, M., Haught, J.R., and Morrison, H.F., 1983, Experience with the EM-60 electromagnetic system for geothermal exploration in Nevada: Geophysics, **48**, 1090-1101.

# APPENDIX 1. INDUCTION COIL DESIGN

The design of an induction coil for use in detecting significant sferics above the combined electronics and coil noise was initially based on using a sferics spectrum published by Macnae et al. (1984) as a guide to the average expected sferics power expected in a given frequency range. The sferics noise in units of $nV/\sqrt{Hz}$ was compared with the corresponding electronics noise to produce the sferics-to-electronics noise ratio as an indication of the possibility of detecting sferics in a given frequency range with an induction coil of a given area.

The horizontal components of the noise are a factor of about 10 greater than the vertical component. However, even for the horizontal components of the noise, the above calculations show that with the present SIROTEM roving vector receiver (RVR-3C), sferics noise will only be detectable at frequencies above 2 to 5 kHz. To detect sferics at lower frequencies, coils with a greater passive area are required. These coils need to be wound to minimise coil noise, and if possible the electronics noise should be minimised with appropriate components.

Figure A1.1 shows the horizontal-component sferics noise compared with electronics and coil noise in the frequency range of 10 Hz to 1 kHz for a $10^4$ $m^2$ coil as used in an RVR-3C. The sferics noise detected by an induction coil was calculated from values given by Macnae et al. (1984). It is seen that the sferics noise is a factor of 10 to 30 greater than the electronics noise in the frequency range of 10 to 100 Hz, and should be detectable at this frequencies. In summer, when sferics activity is expected to be higher, the plotted sferics-to-electronics ratios can be expected to be even higher.

Since the vertical component of the sferics noise is a factor of about 10 lower than the horizontal components, the area of the induction coil has to be increased by a

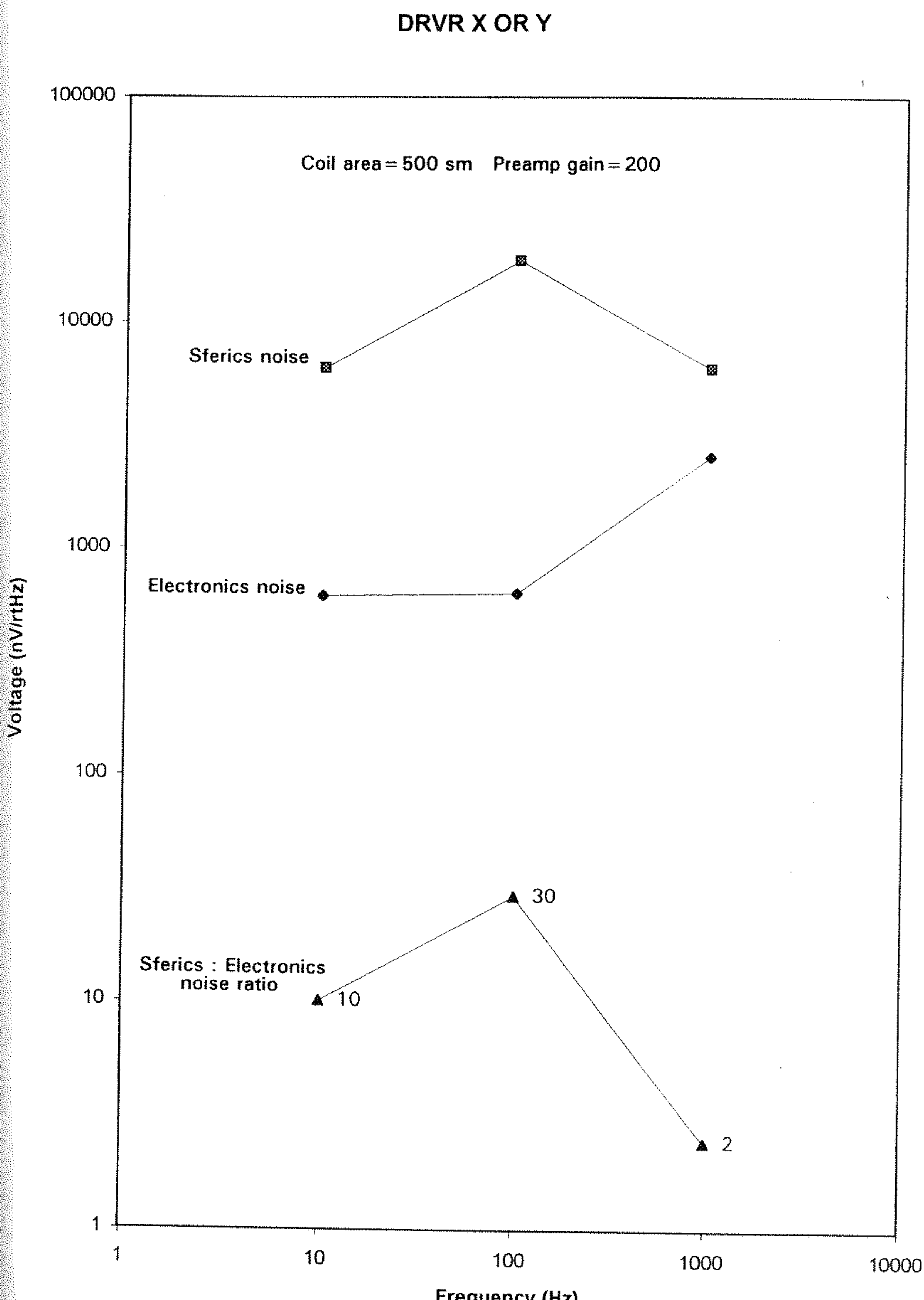


Figure A1.1 Sferics and electronic noise for a horizontal-component induction coil with an area of $10^4$ m$^2$.

factor of at least 10 while keeping the coil noise as low as possible. Since this construction would produce an extremely heavy coil, it is not practical to use coils to measure the vertical component of the sferics noise. A large loop is used instead of a multi-turn coil. Figure A1.2 shows the sferics noise (labelled 'signal' on the diagram) detected with a 100-m loop compared with electronics noise for two different types of preamplifiers (FET and bipolar). Since a loop of wire is used as the sensor, there is no contribution to the electronics noise by coil noise (unlike the electronics noise plotted for the coil in Figure A1.1).

For simplicity, the sferics-to-electronics noise ratio for a 100-m loop is plotted separately in Figure A1.3 as a function of frequency. For the bipolar electronics now used in the preamplifiers of the noise measurement system, this ratio varies from 12.6 to 38 in the frequency range of 10 Hz to 1 kHz, demonstrating that low-frequency sferics should be detectable with a 100-m loop. Since such a loop is usually laid out using twin-flex wire, a two-turn 100-m loop is readily useable for these measurements, and the values of the sferics-to-electronics noise ratio would be double the values shown in Figure A1.3.

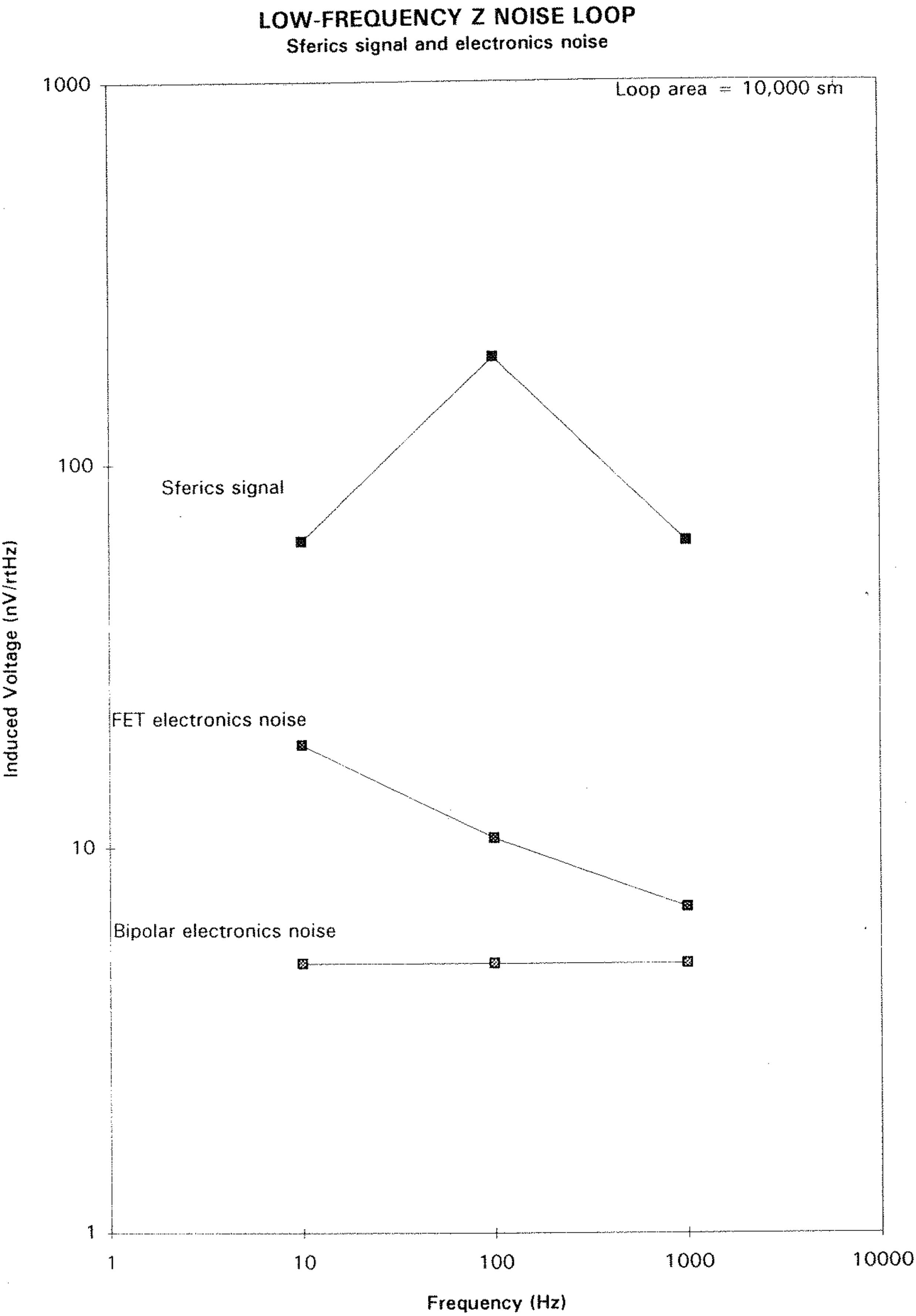


Figure A1.2 Sferics and electronic noise for a $10^4$ $m^2$ loop used to measure the vertical component of sferics noise

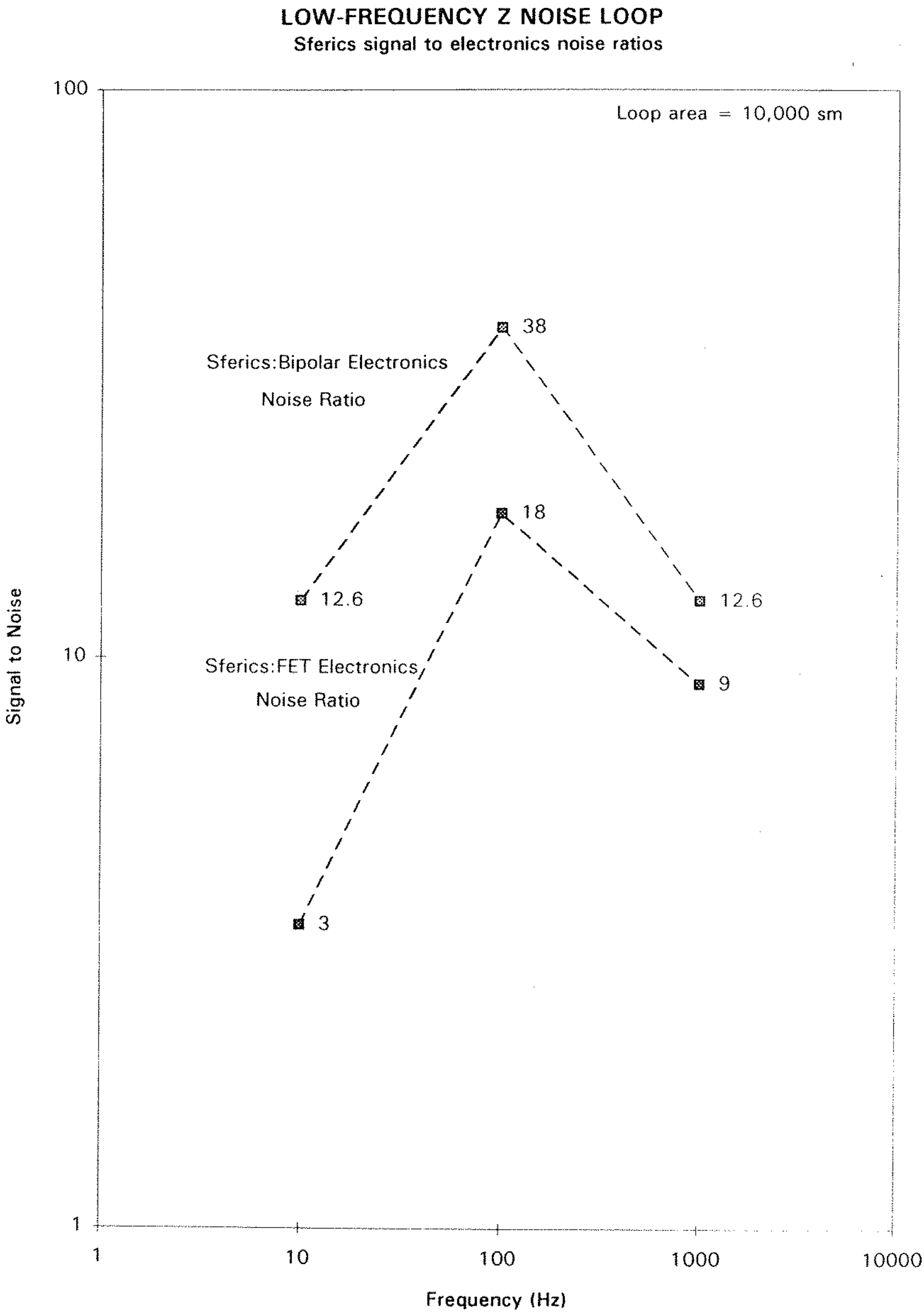


Figure A1.3 The ratio of sferics and electronic noise for a $10^4$ $m^2$ loop used to measure the vertical component of sferics noise.

# APPENDIX 2. MATHEMATICAL FUNCTIONS FOR MEASURES OF CORRELATION

## A2.1 Cross-correlation function

The normalised cross-correlation function, $\phi_{gh}(\tau)$ is given by:

$$\phi_{gh}(\tau) = \frac{\sum_{k=0}^{n-1} g_k h_{k+\tau}}{\left[\sum_{k=0}^{n-1} g_k^2 \sum_{k=0}^{n-1} h_k^2\right]^{1/2}} \ , \ \tau = -(n-1), \ \cdots, \ -1, \ 0, \ 1, \ \cdots, \ n-1 \quad , \qquad \text{(A2.1)}$$

where, $n$ is the number of samples.

## A2.2 Power spectrum

The power spectra, $G(f)$ and $H(f)$, of the time series, $g(t)$ and $h(t)$ are obtained by applying the FFT to each of the time series as follows:

$$G(f) = \frac{1}{n^2}\left|FFT\left[g(t)\right]\right|^2 \qquad \text{(A2.2)}$$

and

$$H(f) = \frac{1}{n^2}\left|FFT\left[h(t)\right]\right|^2, \qquad \text{(A2.3)}$$

where, the number of samples, $n$, in the input time series is a valid power of two, $n=2^k$ for $k$=1, 2, 3, ...., 23.

## A2.3 Cross-power and cross-phase spectra

The cross power spectrum, $S_{gh}(f)$ is given by:

$$S_{gh}(f) = \frac{1}{n^2} G^*(f)\, H(f) \,, \tag{A2.4}$$

where, $n=2^k$ for $k$=1, 2, 3,......, 23 and is the number of samples that can accommodate both time series, $G^*(f)$ is the complex conjugate of the FFT of $g(t)$, and $H(f)$ is the FFT of the time series, $h(t)$.

The cross phase spectrum, $\phi_{gh}(f)$ is given by:

$$\phi_{gh}(f) = \tan^{-1}\left[\frac{\mathrm{Im}\{S_{gh}(f)\}}{\mathrm{Re}\{S_{gh}(f)\}}\right]. \tag{A2.5}$$

### A2.4 Squared coherency spectrum

The squared coherency spectrum, $K(f_j)$, between two time series, $g(t)$ and $h(t)$ at a frequency, $f_j$, is given by:

$$K(f_j) = \frac{\left|S_{gh}(f_j)\right|^2}{\left|S_g(f_j)\right| \times \left|S_h(f_j)\right|} \,, \tag{A2.6}$$

where, $S_g(f)$, $S_h(f)$ are power spectra of the two time series, $g(t)$ and $h(t)$, respectively, and $S_{gh}(f)$ is cross spectrum of $g(t)$ and $h(t)$.

### A2.5 Power coherency number

For a given block of data, if $S_{gh}(f_j)$ and $K(f_j)$ are the cross power spectrum and squared coherency spectrum, respectively, the power coherency number, $C$ is defined as:

$$C = \frac{\sum_j S_{gh}(f_j)\, K(f_j)}{\sum_j S_{gh}(f_j)} \,. \tag{A2.7}$$

A value of $C$ may be calculated when the two time series, $g(t)$ and $h(t)$ are recorded for a given component at two separated stations, or when they are recorded for two components (e.g., the X and Z components) at the same station.

### A2.6 Time shift

Assuming that two time series, $g(t)$ and $h(t)$ are recorded simultaneously at the local and remote receivers, respectively, and one time series is identical to the other with a time shift between two stations of $\tau$, the mathematical relationship between the two time series is given as:

$$g(t) = h(t+\tau). \tag{A2.8}$$

The FFT of Equation (A2.8) is given by:

$$\sum_{t=0}^{n-1} g(t) e^{jt\omega} \Delta t = \sum_{t=0}^{n-1} h(t+\tau) e^{jt\omega} \Delta t \tag{A2.9}$$

or

$$\sum_{t=0}^{n-1} g(t) e^{jt\omega} \Delta t = e^{-j\tau\omega} \sum_{t=0}^{n-1} h(t+\tau) e^{j(t+\tau)\omega}, \tag{A2.10}$$

where $\omega$ is $2\pi f$.

Therefore, the FFT of the time series, $g(t)$, is given by:

$$G(\omega) = e^{-j\tau\omega} H(\omega). \tag{A2.11}$$

By multiplying Equation A2.11 with $H^*(\omega)$, the complex conjugate of the FFT of $h(t)$, Equation A2.11 is written as:

$$G(\omega)H^*(\omega) = e^{-j\tau\omega} |H(\omega)|^2 \tag{A2.12}$$

or

$$G(\omega)H^*(\omega) = e^{-j\phi_{gh}(\omega)} |H(\omega)|^2. \tag{A2.13}$$

According to Equations A2.12 and A2.13, the time shift between the two time series is given as:

$$\phi_{gh}(\omega) = \tau\omega$$

or

$$\phi_{gh}(f) = 2\pi\tau f \,. \qquad \text{(A2.14)}$$

Therefore, The time shift, $\tau$, between two time series is determined by the slope of cross phase spectrum, $\phi_{gh}(f)$, on the plot of $\phi_{gh}(f)$ and $f$.